International Journal of Engineering &Technology, 7 (4) (2018) 6810-6821

International Journal of Engineering & Technology

Website: www.sciencepubco.com/index.php/IJET
doi: 10.14419/ijet.v7i4.24717
Research paper

Survey study on outdoor wideband system propagation of millimeter wave at 28-ghz in a 5g network system

Abdusalama Daho [1] *, Tharek Abd Rahman [1], Ahmed M Al-Samman [1], Youshihde Yamada [2]

[1] Faculty of Engineering, Wireless Communication Centre, Universiti Teknologi Malaysia, Johor Bahru, Malaysia
[2] Department of Electronic Systems Engineering (ESE), Universiti Teknologi Malaysia, Johor Bahru, Malaysia
**Corresponding author E-mail: abdusalamautm2017@gmail.com*

Abstract

High data rates up to 10 Gbps required on fifth generation (5G) wireless communication systems have targeted propagation studies of wireless channels with large bandwidths in millimeter wave spectrums of 28 GHz. Propagation studies cover the measurement, characterization and modelling of wireless channels that are used for testing and enhancement of 5G wireless communication systems. This study aims to contribute to this field by studying the radio wave propagation at 28 GHz for tropical regions, such as Malaysia. The work of this study included measuring, characterizing and modelling wideband channels for 5G wireless communications at the 28 GHz band. Extensive wideband channel measurement campaigns were conducted, to cover the outdoor environment in line-of-sight (LoS) and non-line-of-sight (NLoS) scenarios. Post-processing was also performed using SystemVue and MATLAB software to extract the power delay profile, path loss, angle of arrival (AOA) and root mean square (RMS) delay spread for every considered scenario to characterize the 5G channel. To make a more reliable and easier 5G channel characterization, the powerful propagation simulation, Wireless in Site software was also utilized to investigate all 5G-channel parameters and compare the simulation results with the measurement results. The findings from this study will contribute to the body of knowledge in this field through the development of a proposed model for the 5G channel in Malaysia at the 28 GHz band for the 5G system. Lastly, due to heavy rain in tropical regions, i.e. Malaysia, the wireless channel at high-frequency band should be further investigated in high rainfall regions to include measurement campaigns with different rain rate to investigate the signal degradation, power delay profile and delay spread with rain and compare it with clear air.

Keywords: *5G; Wideband; Millimeter-Wave; 28 GHz; Outdoor Environment.*

1. Introduction

1.1. Background

Technological developments and the rapid evolution and advancement of the wireless and mobile industry took place during the 1970s. Since then, a majority of these wireless mobile technologies have undergone several improvements and evolutions [1], i.e., the 1st generation, 1G; 2nd generation, 2G; 3rd generation 3G and 4th generation, 4G [2]. 1G was introduced during the 1980s as the analogue telecommunications standard; 1G mobile systems used analogue transmissions for speech services. 2G digital telecommunications replaced 1G launched in the late 1990s as a digital mobile telephony technology. 2G initially operated as the global system for mobile communications (GSM) systems, mainly for voice communications. However, 2G technology was soon upgraded to a 2.5G system; with the incorporation of a component, technology known as the general packet radio service (GPRS) as the main feature that distinguished typical 2G networks. The architecture from 2.5G included packet switching and circuit switching, which enabled it to achieve better data rates [3]. Furthermore, the Universal Mobile Telecommunication System (UMTS), which was initially developed for providing a general transport service platform for the 3G internet protocol systems, applied Wideband-Code Division Multiple Access (W-CDMA) technology for delivering enhanced throughput and better spectral efficiency for all wireless network operators [4]. With the continued rapid growth in traffic volume, of mobile data and multimedia applications, such as interactive gaming, internet browsing, and the streaming of audio and video content, the need to increase the capability of existing wireless systems became a prominent issue. This led to the development and launch of the 4G wireless system from the 3G, Long Term Evolution (LTE) and the worldwide interoperability for Microwave Access (WiMAX) systems. The LTE system is designed as an all- internet protocol (IP) based system that offers robust support, for the ever-growing traffic volume of mobile data, with improved system coverage, enhanced System capacity, and high performance; regarding low access, latency, flexible bandwidth, higher data rate, and seamless backward compatibility with other existing radio communication technologies [5]. LTE Advanced (LTE-A), an extension of LTE, added Carrier aggregation and coordinated multipoint technologies to boost system spectral efficiency and overall system performance. LTE-A can support the data rate up to 100 Mb/s for higher mobility access and a data rate up to 1 GB/s for lower mobility wireless access [5]. In summary, from 2G mobile communication systems to 4G systems, wireless mobile technologies have undergone a phenomenal evolution; ranging from a typical telephony system to a communications system capable of transporting rich multimedia content in the same manner as wired networks. Nowadays, the demand for higher mobile data rates and high-speed data transmission is increasing rapidly. If wireless technology needs to provide a higher data transmission rate, the system requires a larger bandwidth and im-

plementation of other innovative technologies. Due to an increase in the wireless traffic data and the rising demand for higher transmission speed, it is important to understand the relationship between a spectrum shortage and a higher capacity. For balancing the association between these significant performance issues, researchers need to reconsider mobile broadband technologies. Furthermore, mobile broadband networks need to be optimized for improving the probability of satisfying the increasing demands of customers for a higher data rate. This optimization would also help in managing the predicted exponential increase in wireless traffic volumes. To achieve greater capacity, a larger bandwidth is needed; hence, the need to look beyond the currently used 3 GHz spectrum band. The Super High Frequency (SHF) band includes the 3-30 GHz spectra; whereas the Extremely High Frequency (EHF) band includes the 30-300 GHz spectra. As the radio waves existing in the SHF and the EHF bands display similar propagation features, the 3-300 GHz spectrum is known as the millimeter-wave (mm-wave) band and possesses a wavelength value ranging between 1 and 100 mm [6]. At present, the existing below 6 GHz frequency spectrum cannot fulfil the future requirements, indicating that new spectral allocations within the mm-wave frequency bands above 6 GHz are necessary for alleviating the existing spectrum shortage. This was the prime reason which led to the development of the 5th Generation (5G) wireless technology [7]. Some researchers have predicted that this 5G mobile network could easily support the increasing traffic data, as it requires low energy consumption and offers a better Quality of Service (QoS). For improving the development of 5G Technology, these researchers have also identified some important processes like the mm-wave and the Multiple-Input Multiple-Output (MIMO) [8]. During the past few years, many studies which have been conducted in the field of wireless communication systems showed a gradual shift from the use of UHF frequencies (300 MHz to 3 GHz) to microwave spectral frequencies, like the mm-wave spectra. Furthermore, much research has been conducted on the use of the mm-wave frequency bands, like 28 GHz. However, the unavailability of steerable antennas and inexpensive electronics has limited the application of many novel technologies like the point-to-multipoint radio wave propagation [9]. On the other hand, many academic and industrial research studies have investigated the probability of implementing 5G technology with the help of microwaves in the frequency band > 6 GHz [10]. To meet these requirements, 5G needs to deal with many challenges; such as supporting the increasingly high data rate, connecting numerous devices, reducing energy consumption and computation load, and establishing secure and reliable communications. Here, the frequency spectrum resource is the major concern for solving these challenges. Hence, 28 GHz and mm-wave bands are the keys to resolving this issue.

To design current and future wireless communications systems, the study of wireless channel characteristics is important. This is because channel behavior may vary over very short spatial distances travelled by signals from the transmitter or receiver terminal. In addition, future backhaul and cellular networks have to take into account the channel propagation and characterization of the microwave and the mm-wave frequencies for developing a reliable and accurate 5G design.

1.2. Problem statement

Understanding the propagation characteristics of wireless is a crucial part of improving the performance of wireless communication systems. Wireless data traffic has been rapidly increasing which implies that huge bandwidth is required to support the large capacity. To address this demand, the wireless industry is moving to 5G cellular technology that will use mm-wave frequencies. However, it is necessary to have a good knowledge of the propagation channel characteristics across mm-wave bands before an accurate and reliable 5G system design can be utilized effectively. Currently, the most candidate frequency for 5G is 28 GHz, which has high bandwidth and less attenuation based on several previous studies in microwave link at 28 GHz.

In this proposal, three challenges of characterizing and modelling wireless channels at 28 GHz are addressed. First, the outdoor environment in tropical regions like Malaysia needs further study regarding 5G wireless channel propagation at 28 GHz. Second, to provide an accurate prediction model, extensive measurement should be conducted to include the structure and effect of the environment and the heavy rainfall conditions in tropical regions in urban areas. Third, conducting a power delay profile study is very important for the wideband channel; implying that the wideband channel measurements are needed using a different angle of arrival. Hence, time dispersion and angular dispersion are required for a 5G channel model without rain and with different rain conditions, especially at extremely heavy rainfall conditions. Notably, only a few measurements have been conducted at 28 GHz for 5G systems, especially in outdoor environments in tropical regions like Malaysia.

1.3. Objectives

The main objective of this proposal is to characterize and model the 5G channel at 28 GHz based on different real measurements and will be achieved through the following:

i) To investigate the 5G channel in terms of propagation path loss, power delay profile, delay and angular spreads and rain attenuation effects based on extensive wideband measurements.
ii) To propose prediction models for the 5G channel at tropical regions.
iii) To verify and evaluate the proposed model by comparison of measurement and simulation.

1.4. Scope of research

The scope of this research consists of the following:

- 5G channel characterizations will be investigated based on different measurement campaigns.
- The wideband (WB) measurements will be carried out using a 5G channel sounder with high resolution of 1 ns.
- All measurements are conducted under the single-input-single-output (SISO).
- The recommended bandwidth for a 5G system of 1 GHz will be used.
- The potential candidate frequency for a 5G system, of 28 GHz will be used.
- The measurement will be conducted in an outdoor environment within an urban area.
- Different line of sight (LOS) and non-LOS (NLOS) scenarios will be investigated.
- The rain attenuation effects for path loss, power delay profile as well as delay spread will be investigated.

2. Literature review

2.1. Introduction

Wireless communication has become quite common nowadays due to significant technological advancements. Wireless communication provides media that transforms our work, education, and entertainment, and is expected to connect everything, anywhere and at any time using a 5G system [11]. Given the vast bandwidth now available at millimeter wave (mm-wave) bands, 5G wireless networks will use potential frequencies in the mm-wave band. The most candidate bandwidth is 28 GHz based on recent studies. Therefore, the propagation study at the 28 GHz band in different environments is required to investigate the wireless channel propagation in this band for the 5G system.

2.2. 5G network systems

Cell phones have quickly become a modern-day necessity. Along with making/receiving phone calls, current smartphones consist of cameras, sensors, web browsers and multimedia infotainment, etc., which has increased the usage of cell phones and users alike. In supporting this subscriber base, the telecommunication industry must periodically upgrade its technology and carry out technological innovations to fulfil the demands of users [12]. In this case, the current 4G network would be superseded by 5G, which highlights the paradigm shift in the mobile network. As reported by many industrial and academic committees, the 5G system will be on 2020 for providing global connectivity. Many technologies are presently being investigated for 5G systems, such as SISO, Multiple-Input Multiple-Output (MIMO), Vehicle-to-Vehicle (V2V), High-Speed Train (HST), and mm-wave communications [12]. These technologies introduce new propagation properties and specific requirements on 5G channel modelling. Importantly, 5G systems will help to access and share data in low latency and high data rate environments as described in the following subsection.

2.2.1. 5G requirements

The International Telecommunication Union (ITU) coordinates the shared global use of the radio spectrum and develops technical standards for the seamless interconnection of networks. The ITU designed the IMT-2020 speciation [13 - 16]. Figure 1 shows the 5G key goals and key performance indicators. The new demands and performance indicators for the 5G network are next discussed.

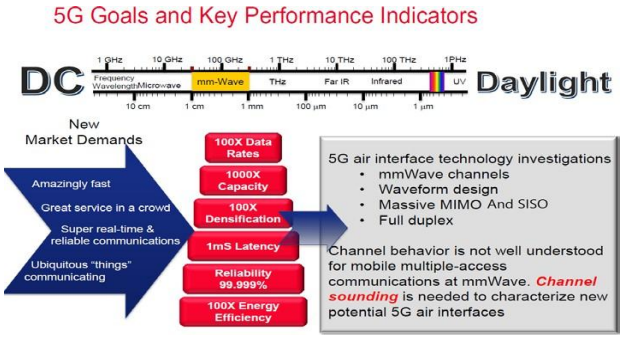

Fig. 2: 5G goals and key performance indicators.

- Data Rate:

5G systems provide an 'aggregate data rate' (or area traffic capacity), i.e., the data served by a network in bits/s/unit area. Also, it should provide a data rate of 20 Gbps (downlink) and 10 Gbps (uplink). Urban and semi-urban users will experience a 100 Mbps (downlink) and 50 Mbps (uplink) data rate. 5G will support mobile consumers (mobility ≤ 500 km/h)[14].

- Large Bandwidth:

Mm-wave is a promising 5G technology [17] which has a large bandwidth and a data rate of hundreds of Gbps. Higher frequency propagation causes path loss (PL). However, mm-wave systems with small cells (100–200 m radii) display a satisfactory performance. A high PL is overcome by beam forming, which combines the MIMO technologies. A high-gain steerable antenna array transmits or receives signals in specific directions, bypasses obstructions, and overcomes PL [18]. In this work, 1 GHz bandwidth at 28 GHz band will be used for the 5G channel propagation study. The path loss will be investigated using a SISO system and the rotator system used to study the signal at a different angle to emulate the beam forming technique.

- Latency:

User plane latency is defined as the network contribution from the transmission of a packet to its reception (in ms). 5G systems require a latency of 1 ms for various applications such as an autonomous car, robotic arm, remote surgery and internet of things (IoT) applications [14].

- Spectrum Efficiency:

Due to frequency (spectrum) scarcity, new technologies must transmit a higher bit rate for the same resources. 5G systems provide 3 times higher bits/sec/Hz than 4G [14].

- Energy Efficiency:

This refers to the information, i.e., bits transmitted/received from users, per energy consumption unit. Energy efficiency is measured (bit/Joule) in a radio access network. It also refers to the information (bits/ unit energy consumption) in the communication module. As the aggregated data rate in a 5G network is 100 times higher than 4G, the energy efficiency must increase by 100 times to maintain constant energy consumption [14].

- Connection Density:

The IoT aims to provide constant connectivity to various devices for improving mobile applications. 5G networks are envisaged to support a connection density of ≈ 106/km^2

- Cost:

With increasing 5G data rates, there would be a proportional decrease in the cost/bit.

- Massive MIMO:

The traditional wireless SISO devices possess a single antenna for accessing radio signals. However, MIMO devices have multiple antennas. In a rich scattering, of a radio-wave propagation environment, every antenna pair acts as an independent channel. Hence, the data rate can be increased using massive MIMO without increasing the transmission power.

2.3. Wideband channel

Wideband systems, like LTE and LTE-A and future 5G use bandwidths up to 20 MHz, 100 MHz and 1 GHz, respectively. This implies that they can differentiate between the multipath components (MPCs) by resolvable delay bins. Hence, every delay bin consists of MPCs, which cause a fading of each separate bin. However, the resolvable MPCs can be considered as frequency flat, and the impulse response can be defined using the Dirac delta function (δ function) as in [19]:

$$h(\tau) = \sum_i^{L-1} \alpha_i \, \delta(\tau - \tau_i), h(\tau) = \sum_i^{L-1} \alpha_i \, \delta(\tau - \tau_i) \quad (2.1)$$

Where α_i and τ_i are the $i-th$ path gain and delay, respectively, the L is the number ofpaths.

2.4. Millimeter wave band (mm-wave)

Development of communication technologies and mobile devices has led to an ever-growing demand for higher capacity. 4G LTE systems will face this increasing trend, leading to network congestion by 2020. Every technology has a life cycle of ≤ 10 years. For 5G wireless networks, the academic and industrial researchers propose a wireless technology, which offers multi Gbps and uses steerable horn antennas and mm-wave spectra. However, the 5G channel propagation in the mm-wave band using steerable horn antennas needs extensive study in order to understand the wideband wireless channel behavior.

2.5. Multipath channel propagation

Multipath propagation occurs if the signals propagate between the source and destination by bouncing off various Interacting Objects (IOs). Every signal echo undertakes a different propagation path from the source to the destination, called the multipath component (MPC). The wireless system consists of 3 main components, the transmitter (Tx), a wireless channel and a receiver (Rx) as shown in Figure 3: In a typical environment, the electromagnetic waves travel from Tx to Rx through different paths due to reflection, diffraction and scattering. The electromagnetic field superimposes the LOS and reflected paths in an MPC.

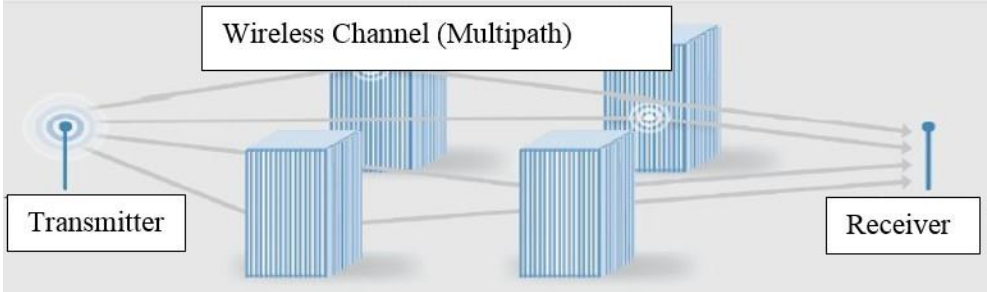

Fig. 4: Multipath propagation concept.

At the receiver side, the total received signal is received which can distinguish between different paths using a different technique. For measurement, the wideband channel sounder with high resolution is used to resolve each multipath component with different propagation time delay. Different parameters should be investigated to fully understanding the wireless channel behavior in any particular wireless communication system, which includes path loss, power delay profile, and root mean square delay spread (RMSD). The environment plays a crucial role in wireless channel propagation that depends on several parameters such as the type of environment, building structure and the rain rate in the environment.

2.6. Channel measurement techniques

Different channel measurements, similar to the narrowband and wideband techniques, help in studying the Radio Frequency (RF) channel, based on their bandwidth and channel delay spread. Narrowband techniques measure the PL, narrowband fading and Doppler spread. However, in this case, the received signal refers to the vector summation of MPCs, without providing any quantitative multipath data. For high signal bandwidth, wideband techniques measure the time dispersion, PDP, and RMS-DS. Wideband techniques use channel sounders for resolving MPCs and measure the propagation delay parameters. The bandwidth signal increases the symbol rate, indicating that the channel was frequency-selective; hence, the time delay spread cannot be neglected [20]. In this work, a wideband signal correlation sounder system is used to measure the 5G channel at 28 GHz. A hardwired signal between Tx and Rx is unnecessary in this case because the signal contains a rubidium synchronizations clock that synchronizes the Tx and Rx wideband signal at 28 GHz.

2.7. Related work

In this section, previous studies carried out at the 28 GHz spectra are reviewed.

Zhao et al. (2013) [21], presented the reflection coefficients and penetration losses using a 28 GHz millimeter wave (mm-wave) system for conventional building materials, like tinted glass, clear glass, brick, concrete, and drywall in New York (NYU) City. They implemented the 400 Mega chips per second (Mcps) sliding correlate channel sounder and steerable horn antennas (24.5 dBi) for designing the mobile devices, with adaptive antennas. The outdoor building materials showed a maximal reflection coefficient of 0.896 for tinted glass, compared to the less-reflective indoor building materials. The researchers noted that the penetration loss depended on the number of obstructions, the distance between the Transmitter (Tx) and Receiver (Rx), and the surrounding environment. The interior office walls showed the highest penetration loss of 45.1 dB, as the Tx-Rx distance was 11.39 m.

Azar et al. (2013)[22], used the 400 Mcps channel sounder with directional horn antennas for measuring the characteristics for the mm-wave systems in urban environments. They conducted 28 GHz outdoor propagation measurements in Manhattan, for 3 base stations and 75 receiver locations, over a distance of 500 m. They measured the Path Loss (PL) as the function of the Tx-Rx distance, angular distribution of the received power using directional antennas (24.5 dBi), and power delay profiles (PDPs) in NYU City. They observed many resolvable multipath components in NLOS and LOS environments, with a multipath excess delay spread (20 dB) of 1388.4 ns and 753.5 ns, respectively. The diverse spatial channels indicated that the mm-wave systems with electrically-steerable antennas could exploit the resolvable multipath components for creating viable links for the cell sizes of 200 m.

In a separate study, Samimi et al. (2013)[23], measured the propagation values at 28 GHz in New York City, using 4 Tx and 83 Rx locations, at 500 m. They used a 400 Mcps channel sounder with steerable 24.5 dBi horn antennas for the Tx and Rx for measuring the angular distribution of the multipath power for various propagation distances and urban settings. They studied the small-scale fading of the closely-spaced PDPs at half-wavelength (5.35 mm) increments and a small-scale linear track (10 wavelengths, or 107 mm) at 2 Rx locations. In this study, they proposed a novel lobe modelling technique for creating a statistical channel model for the lobe PL and shadow fading. The researchers noted that the urban environment in NYU City has a multipath-rich environment, which used highly-directional steerable horn antennas. An average of 2.5 signal lobes existed at any Rx location, wherein every lobe showed a total angle spread of 40.3° and an RMS angle spread of 7.8°.

Rappaport et al. (2013) [24], stated that bandwidth shortage affecting wireless carriers led to the investigation of the mm-wave spectra for future cellular networks. Here, the researchers exploited novel mm- wave cellular systems, methodologies and hardware. Various measurements values indicated that the 28 and 38 GHz frequencies could be used when they employed steerable directional antennas at the base stations and mobile devices.

In another study, Sulyman et al. (2014)[25], used the mm-wave spectra for determining the empirical PL models, based on an arbitrary pointing angle of directional antennas. According to the network simulations, 3- times more base stations were needed for accommodating the 5G network (cell radii up to 200 m) compared to the 3G and 4G systems (cell radii of 500 m-1 km). However, when they pointed the antennas in the base station and mobile direction, the coverage range improved, with no interference, which reduced the number of 5G base stations. The researchers noted a 20-times higher capacity for random pointing angles, compared to the 4G Long Term Evolution (LTE) networks, which improved when they used beam-combining techniques and pointed the antennas in the strongest Tx and Rx directions.

Nie et al. (2014)[26], applied the mm-wave technique for analyzing the signal outage at 28 and 73 GHz, using spread spectrum sliding correlate channel sounders with high gain, directional steerable antennas in NYU. They used 3 identical Tx locations for the 28 and 73 GHz campaigns, whereas the 73 GHz campaign included 2 novel Tx locations. The researchers tested 25 Rx locations for each of the 3 Tx locations in the 28 GHz campaign; and 27 receiver locations for the 5 Tx locations in the 73 GHz campaign. In total, they tested 75 Tx- Rx location combinations at 28 GHz and 74 Tx-Rx combinations at 73 GHz, wherein the T-R distance was up to 425 m. They also noted a maximal transmission power of 30 dBm at 28 GHz and 14.6 dBm at 73 GHz and observed the estimated outage probabilities of 14% and 17% at 28 and 73 GHz, respectively, and 16% for the 73 GHz scenario.

Akdeniz et al. (2014)[27], measured the values at 28 and 73 GHz in New York, and developed spatial models, for channel parameters, like PL, number of spatial clusters, angular dispersion, and outage. These models were used for assessing the mm-wave micro- and Pico- networks in urban environments. They detected strong signals at a distance between 100 and 200 m from potential cell sites, even in the NLOS environments, using multiple clusters that supported spatial multiplexing. The researchers concluded that the mm-waves showed a higher capacity than the 4G networks, without increasing the cell density from the urban deployment.

On the other hand, Deng et al. (2014)[28], used the wideband mm-wave and a 400-750 Mcps sliding correlate channel sounder, with steerable directional horn antennas, present at the Tx and Rx ends for measuring the mm-wave channels in New York. The NYU WIRELESS research Centre, i.e., NYUSIM, carried out several propagation measurement campaigns in indoor and outdoor environments at the 28 and 73 GHz bands, which helped in developing directional and omnidirectional PL models, presented in the study. This study presented the values for the directional PL, omnidirectional PL and RMS delay spread, which could help in developing and standardising the novel mm-wave wireless networks.

Sun et al. (2016)[29], used the mm-wave for the urban microcellular and indoor office scenarios, at 28 GHz and 73 GHz, and investigated different PL models, i.e., a single frequency Floating-Intercept (FI) model, single-frequency Close-In (CI) free space reference distance model, multi-frequency Alpha-Beta-Gamma (ABG) model, multi-frequency CI model, and multi-frequency CI model with a Frequency-weighted PL exponent (CIF), in the LOS and NLOS environments. The researchers noted that the CI and CIF models offered better estimation and stable frequencies and distances, which showed a good physical basis and low computational complexity, compared to the FI and ABG models. Also, the PL in an external scenario showed low dependence on frequency, while the PL increased with frequency and free space PL in indoor environments. The CI model was better for outdoor environments, whereas the CIF model was better for indoor modelling. This study indicated that the CI and CIF models used fewer parameters and offered better closed-form expressions, without compromising the model accuracy, compared to the 3GPP and WINNER PL models.

According to Kim et al. (2016)[30], many studies used highly directive antennas or beam forming processes, with large array antennas for establishing a reliable link between the Tx and Rx, for overcoming the PL on the high-frequency bands. The researchers introduced an outdoor channel measurement, which used the directional horn antenna in the 28 GHz frequency band, in low-rise and high-rise Korean environments. The researchers derived empirical models for extracting RMSDS and the angular spread of arrival corresponding to the beam width of the antenna, for studying the multipath characteristics.

Al-Samman et al. (2016)[31], described time dispersion parameters and PL models for candidate frequencies > 6 GHz including 28 GHz for the closed outdoor environment. They compared the single- frequency and multi-frequency schemes of the CI, FI and ABG models. The researchers proposed a novel PL model which accounted for Frequency Attenuation (FA) with distance, called the FA-PL model. Here, the researchers introduced a frequency-dependent attenuation factor, XF(f), which added the CI reference attenuation. They carried out ultra-wideband measurements for various frequencies (between 10 and 40 GHz) for the LOS and NLOS scenarios. The researchers estimated the RMSDS, mean excess delay and maximal excess delay.

Junghoon et al. (2016)[32], introduced a novel channel measurement system, with time synchronization, i.e., a sliding correlate channel sounder, which used 250 Mcps PRN sequences. This system helped in observing the behavior of 28 GHz wave propagation and formed novel narrow beams in specific directions (classical narrow beam-forming). This synchronized system analyzed the wideband channel characteristics. The researchers also carried out outdoor channel measurements for foliage effects, signal outage, PL and outdoor-to- indoor conditions. They interpreted the spatial channel modelling for Omni-like values with temporal characteristics after analyzing channel modelling parameters, like RMSDS, a number of clusters, excess delay, PDP, and angular spread. The results showed that the average cluster number was 2.41 ± 1.44. The average RMSDS was 36.06 ± 46.73 ns whereas the mean RMS azimuth spread for the angle of departure and arrival were 6.65° and 24.04°, respectively.

Rajagopalan and Hoffman (2016)[33], used a statistical model for simulating an urban environment with diverse building distributions for studying the mm-wave spectra propagation in urban environments. Extensive simulations were conducted for analyzing the PL behavior for LOS and NLOS conditions in 28 GHz and 73 GHz mm-wave frequencies. The PL showed a logarithmic fit for the LOS and NLOS environments. Their simulations showed that the omnidirectional free space PL is ≈ 30 dB higher for the mm-wave than the existing 3GPP cellular systems. The researchers proposed using highly-directional horn antennas with beam formation for decreasing the PL.

In a study by Naderpour et al. (2016)[34], they investigated the channel sounding in a campus street canyon at 15, 28 and 60 GHz in backhaul scenarios and noted that the PL exponent is close to the free space in LOS, while an additional 5-30 dB loss was seen in NLOS. Furthermore, an azimuth and delay spread < 25° and 30 ns were seen, which decreased with an increasing Tx-Rx distance. The results showed the highest spread values at 28 GHz, especially for long Tx-Rx links, were due to the presence/ absence of vehicles, and the Tx/Rx antenna heights.

Wang et al. (2016)[35], used a ray tracing method for simulating the outdoor characteristics at 28 GHz, determining the PL in LOS and NLOS conditions and compared all results with the 2.6 GHz band. Their results indicated that the PL at 28 GHz was ≈ 20dB in both LOS and NLOS. Compared to the 2.6GHz band, the 28 GHz band showed a smaller delay spread, indicating that it suppressed the inter-symbol interference and offered high transmission rates.

Tuan et al. (2016)[36], applied an advanced design Ptolemy system simulator for RF circuits and a ray tracing simulator for antenna propagation, and compared the performance of the mm-wave beam forming system with a 28 GHz band with different Half-Power Beam Width (HPBW) values (5º, 10º, and 20º) of the base station antennas in an outdoor-to-indoor propagation case. They analyzed the simulation results for the delay spread, PDP, frequency response, and Error Vector Magnitude (EVM). They stated that the EVM of 5º HPB is better than the 10º and 20º HPBW, while the LOS position showed a better EVM than -23 dB, while the direct signals were blocked by concrete pillars or walls for the NLOS conditions. Due to multiple reflections and beam steering, the received signal showed an EVM better than -15 dB.

Lee et al. (2016) [37], investigated the application of the International Telecommunication Union – Recommendation (ITU-R) PL models to the mm-wave bands. They focused on the NLOS conditions (urban street canyon environments, where the radio waves propagated along the street roads, while the building corners were obstructive). For this purpose, they compared the values at 28 GHz in Seoul to two ITU-R PL models, i.e., the ITU-R P.1411 Street Canyon NLOS PL model and the ITU-R M.2135 Urban Microcell (UMi) Manhattan- grid NLOS PL model. They noted that the predictive values of the original ITU-R models deviated from the 28 GHz data. However, they modified a few parameters in the ITU-R P.1411 model and generated better predictions, which were in line with the calculated data. Hence, without modifying the parameter values, the existing ITU-R P.1411 model could be applied to the 28 GHz model.

Hur et al. (2016)[38], compared the values derived from a spherical 28 GHz channel sounder system, implemented in the urban street-canyon environments of Daejeon, Korea and the NYU campus, Manhattan, using ray-tracing simulations. As these scanning measurements were costly and time-intensive, a relatively small number of channel samples were obtained, which were used for

quantifying the ray-tracer accuracy and deriving multiple values for filling the measurement gaps. The researchers presented a set of mm-wave radio propagation parameters based on the values and ray-tracing. The resultant channel model, based on the 3GPP Spatial Channel Model (SCM) methodology, was also described.

In another study, Yan et al. (2016)[39], conducted 28 GHz and 73 GHz outdoor campaigns at NYU University and the 38 GHz and 60 GHz outdoor measurement campaigns at the University of Texas, Austin (UTA) in this study. They included the measurement parameter list, measurement environment description, and measurement results for every campaign, and provided the estimated PL data and map coordinates.

Tang et al. (2017) [40], determined the mm-wave channel characteristics, in an UMi communication scenario at 28 GHz. The researchers analyzed the path number, RMSDS and the mean excess delay. They noted that the path number showed a normal distribution fit, while the RMSDS and mean excess delay showed a good Lognormal distribution fit. They compared these values with other methods and discussed the effect of distance on the path number.

Park et al. (2017)[41], used an mm-wave channel measurement system for investigating the Vehicle-to- Vehicle (V2V) environment at 28 GHz, by installing an omnidirectional antenna for determining the PL and a steerable directional antenna for the multipath characteristics on the Rx side. The campaigns were conducted in open areas for understanding the blockage effects of the vehicles. They analysed the blockage loss characteristics with regards to the different Rx positions and measured the delay and angular spreads, using a correlogram-based multipath component extraction algorithm.

Khatun et al. (2017)[42], presented the simulation results of various 3-D statistical channel models for the mm-wave NLOS communication in Boise. They simulated the power lobe angle of arrival/angle of departure (AOA/AOD) spectra, PDPs, and the PL models for the 28 GHz and 73 GHz bands. They described the directional and omnidirectional PL models for a random sample of 10-500 m distances. The PL models with the 28 GHz and 73 GHz omnidirectional transmissions showed a similar exponential value. Also, the researchers believed that by 2020, the 28 GHz and 73 GHz frequency bands would be used in 5G technology for improving the data rates and spectral efficiency.

Bas et al. (2017)[43], summarised the results from the 3, 28 GHz channel measurement campaigns, i.e., microcellular in a residential area, stationarity region and a dynamic scattering in urban environments, which were carried out using a real-time channel sounder, which performed directionally-resolved channel measurements in dynamic environments.

Zhong et al. (2017)[44], used a channel sounder system with omnidirectional antennas and high gain power amplifiers for analysing the propagation characteristics at 28 GHz and 38.6 GHz. The base station, height-dependent, PL model was derived after channel measurement in NLOS urban outdoor scenarios. They compared the PL models at 28 and 38.6 GHz with the PL model at 3.5 GHz and also compared the PL model with the 3GPP 38.900 model and noted that since the 3GPP had a low PL, it overestimated the system performance.

Azhari et al. (2017)[45], in a separate study, proposed various propagation models for approximating the network's coverage in the areas near Malaysian roads, which were on flat and elevated topographies. The researchers conducted simulation studies for determining the effect of the topography gradient on the PL for different mm-wave bands, using the 3 outdoor PL models, i.e., the CI, FI and ABG models. They investigated 5 mm-wave frequency bands at 28, 32, 38, 46 and 73 GHz, with different gradients and LOS scenarios. Their PL computation, based on the selected models, showed that the topography elevation along the roads caused a < 2 dB deviation than the flat terrain values. However, the model selection affected the precision of the PL model.

Zhou et al. (2017)[46], described a 28 GHz PL model based on the values of the channel measurement campaigns with rotating platforms and directional antennas in indoor and outdoor environments. They noted that the Tx and Rx cover a large range of angles in the azimuth and elevation planes for determining the major propagation paths and measuring burden. With increasing cluster numbers, the PL Exponents (PLEs) increased, while the shadow factors showed an increasing tendency. All clusters showed a low PLE due to their multi propagation paths, while the narrow and long corridors showed a low LOS PLEs compared to the office. Their model considered the cluster characteristics and combined the directional and omnidirectional models within one framework, which improved the 5G model.

Wei et al. (2017)[47], used a ray tracing simulator for analyzing the channel characteristics in the radio wave propagating environment. Here, the researchers calibrated the reflection coefficients of the ray-tracing simulator, based on the values measured in the NYU Manhattan campus at 28 GHz, and also optimized the dielectric constant and loss tangent parameters.

Han et al. (2017)[48], presented the wideband channel characteristics of 28 GHz in an UMi scenario in Beijing. They conducted the omnidirectional-antenna and horn-antenna-based measurements for 800 MHz They determined the shadow fading (σSF) and compared the value to the standard protocol. Unlike the conventional techniques, the σSF was calculated for every value in the single routes. The standard model largely overestimated the σSF of the frequency band in the LOS and NLOS environments. Additionally, the researchers determined the 3D data using the Space Alternating Generalized Expectation-maximization (SAGE) algorithm and estimated the Angle Spread of Arrival (ASA) and Angle Spread of Departure (ASD) at various rotation sites. They noted that the parameter space dimension used in a clustering algorithm affected the results of the recognizable multipath.

Hindia et al. (2017) [49], stated that a majority of the existing channel models could not be applied directly to mm-wave systems due to different band characteristics. Here, the researchers proposed a novel PL model for various mm-wave bands and presented popular channel models and their authentication for the outdoor environments using the 26, 28, 36, and 38 GHz bands. They measured the outdoor LOS and NLOS scenarios at a distance with a separation distance of 114 m between the Tx and Rx antenna locations for comparing the popular and novel PL models. The outdoor channel characterization and modelling were conducted in Malaysian tropical environments, and the results of the models were tested for the single- and multi-frequency schemes. Their proposed model was accurate and straightforward regarding frequency and environment signal attenuation. The PL exponent values were 1.54 and 3.05 for the 20 GHz and 30 GHz bands, respectively.

Lodro et al. (2018)[50], simulated a statistical channel model for the 5G systems, using the statistical channel modelling software, developed by NYUSIM. This simulator handled a wideband of carrier frequencies from 500 MHz-100 GHz for different environments like the UMi, urban macro cell and rural macro cell. It also supported the RF bandwidth from 0-800 MHz, which made it suitable for statistical channel modelling of the 5G systems. Here, the researchers used the operating carrier frequency of 28 GHz and an UMi performance in LOS, based on the directional, omnidirectional and small-scale PDPs.

Jarndal and Alnajjar (2018)[51], proposed an efficient mm-wave propagation model, which displayed better reliability and accuracy for simulating the environment, unlike the popular 2-ray and statistical models. The researchers used the diffraction theory for calculating the multi-reflection–diffraction signals received for the linear and circular polarization. They also derived mathematical formulae for each ray contribution with regards to the building dimensions and distances between the building, mobile and Tx. This model was used for evaluating the performance of the communication systems at 28 and 73 GHz, using the signal fading characteristics and PDP.

Junghoon et al. (2018)[52], conducted 28 GHz outdoor NLOS channel measurements in Pyeongchang, using a synchronous channel sounder system. This model helped in deriving the channel parameters like PL, delay distribution and spread, and the angle distributions and spread. This analysis offered better statistics

for the 28 GHz Omnidirectional channel model. Additional measurement campaigns and analyses have to be performed for deriving a better channel model at 28 GHz.

Lee et al. (2018)[53], studied the channel characteristics and cell coverage of the 28 GHz mm-wave band by developing a 3D ray tracing simulation. They verified the simulation accuracy by comparing the results with actual measurements. They noted a similar PL in the LOS and NLOS regions, while the shadowing factor was different in the NLOS regions. They carried out simulations in downtown Gangnam, a high-rise urban area in Seoul, South Korea. They compared the results derived from the simulated 300 base stations operating in a 900 MHz LTE band. The LOS regions showed that the PL of 28 GHz was 30 dB higher due to the free-space PL gaps, while the PL varied in the NLOS regions because of multipath fading. They also determined the outage probability for understanding the validity of mm-wave cell deployment and coverage for the UMi environments. Lee et al. (2018)[54], studied the propagation of PL characteristics related to the application of high-gain directional beam forming in the mm-wave process, using two aspects. The first aspect involved the beam width effects. Due to the multipath nature of the mobile environments, it was believed that a narrower beam width antenna could capture few multipath signals and increase the directivity gain. The researchers normalized the directivity gain and noted that the narrow beam width reception incurred an additional PL compared to the omni-directional-antenna power reception. They collected the data for 28 GHz and 38 GHz in urban regions and noted that this additional propagation PL was a function of the HPBW. They also observed that significant PL occurred due to a small angle misalignment.

Karttunen et al. (2018)[55], parameterized an excess loss-based MPC cross-Polarization Ratio (XPR) model in indoor and outdoor environments for frequency bands > 6 GHz. They carried out measurement campaigns at 28 GHz. They stated that the conventional MPC-XPR model, which assumed a constant mean value, did not fit their data and overestimated the depolarization effect. They noted that the MPC-XPR was inversely proportional to the excess loss in the free-space PL. This model was better since a high excess loss led to more lossy interactions or an increased interaction with objects, leading to higher depolarization. The MPC XPR was not frequency or environment-dependent and showed a 0 dB excess loss and a mean XPR of 28 dB. This model can be applied to the current models for producing more realistic MPC XPRs for a 6-GHz radio link.

Sheikh and Lempiainen (2018)[56] carried out a multidimensional analysis of the multipath propagation in indoor and outdoor environments at high frequencies, i.e., 15 GHz, 28 GHz and 60 GHz, using 3D ray tracing tool in Yokosuka, Japan. Their 3D ray tracing tool provided the data for the received signal strength, power angular spectrum and PDP. Their simulation results indicated a propagation difference in indoor and outdoor environments at high frequencies and highlighted the diffuse scattering effects at 28 and 60 GHz. In simple outdoor UMi environments, the researchers noted a LOS connection between the Tx and Rx, where the average received signal at 28 GHz and 60 GHz was 5.7 dB and 13 dB less than the signal at 15 GHz. These differences, in the received signals at higher frequencies, were extended in indoor environments due to high building penetration loss. However, this propagation and penetration loss at higher frequency was compensated by using an antenna with a narrow beam width and a large gain.

Table 1: Comparison of Channel Characteristics Path Loss Model Approaches for WB Systems

Researchers	Approach	PL Model	Remark
Hinidia 2017	Measurement outdoor narrow band system LOS and NOLS	The large scale path loss model for the outdoor tropical region	Comparison In order to highlight some of the most recent progress in the field of path loss modelling or channel characterization, three models including CI, FI and ABG are compared for individual Experiments carried out by the researchers in outdoor urban Environment. These
Azhari 2017	Simulation outdoor wideband system LOS	Comparison between ABG, CI and FI PL models at 28 and 73 GHz,	This paper presents simulation studies on the impact of topography gradient towards PL for different millimeter wave frequency bands based on available outdoor PL models. Three outdoor PL models were compared, namely close-in (CI) free space reference distance model, floating intercept model (FI), as well as alpha-beta- gamma (ABG) model. Five-millimeter frequency bands at 28, 32, 38, 46 and 73 GHz with different gradients and line-of-sight (LOS) scenarios were investigated in the simulation.
Al-samman 2016	Measurement outdoor wideband system LOS	To investigated the propagation characteristics of mm-w 5G the PL and Time dispersion CI, FI, ABG.	This paper presents path loss models and time dispersion parameters for different candidate frequencies above 6 GHz for fifth-generation (5G) wireless communications. Three well- known path loss models are compared for single- frequency and multi-frequency schemes: the close-in (CI) free space reference distance model, the floating intercept model (FI), and the alpha-beta-gamma (ABG) model. This paper also proposes a new path loss model to account for frequency attenuation (FA) with distance,

2.8. Research gap

The previous works in tropical region (Table 2) have shown that the wideband channel characterization for outdoor environment in Malaysia at 28 GHz is limited. This proposal will cover this field by studying the radio wave propagation at 28 GHz in tropical region, e.g. Malaysia. It will be devoted to the work of measuring, characterizing and modelling wideband channels for 5G wireless communications at 28 GHz band. Extensive wideband channel measurement campaigns will conduct, to cover outdoor environment in line-of-sight and non-line-of-sight scenarios. The post processing will be performed using SystemVue and Matlab software to extract the power delay profile, path loss, angle of arrival AOA and root mean square delay spread for every considered scenario to characterize the 5G channel. Due to heavy rain in tropical region, i.e. Malaysia, the wireless channel at high frequency band needs to more investigation in high rain rate region. This work will conduct measurement campaigns with different rain rate to investigate the signal degradation, power delay profile and delay spread with rain and compare it with clear air. To make more reliable and easier 5G-channel characterization, the powerful propagation simulation, Wireless In Site software will use to study and investigate all 5G channel parameters and compare the simulation results with the measurement results. Based on measurement and simulation results, this work will develop the general model for 5G channel in Malaysia at 28 GHz band for 5G system.

3. Methodology

3.1. Introduction

In this Chapter, Section 3.2 describes the general framework for this proposal and Section 3.3 presents the research methodology. Sections 3.4 and 3.5 describe the measurement equipment and environment, respectively. The WI software discussion is presented in Section 3.6, followed by presenting the channel parameters in Section 3.7.

3.2. General framework

The general framework for this work is shown in Figure 5. It includes all the steps that will be. Used in this study

Fig. 6: Research framework.

3.3. Research methodology

This section presents the methodology used in performing this work that consisted of three phases as shown in Figure 4 (a), Figure 5 (b) and Figure 6 (c). The channel measurement and environment setup were conducted based on Phase (a). Phase (b) represented the data collection, post-processing, channel characterizations parameters and data analysis. The proposed prediction model for the 5G channel at 28 GHz in the tropical region was performed in Phase (c). This phase included the 5G channel model using Wireless In Site (WI) software and the comparison with the real measurements and the previous models from different research areas.

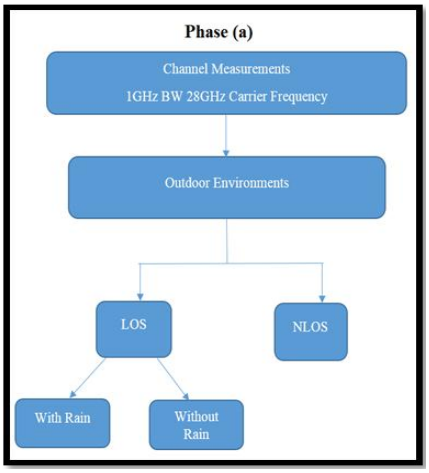

Fig. 7: Flow chart of research methodology - Phase (A).

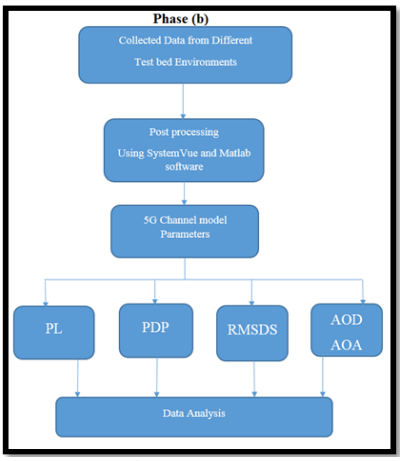

Fig. 8: Flow chart of research methodology - Phase (B).

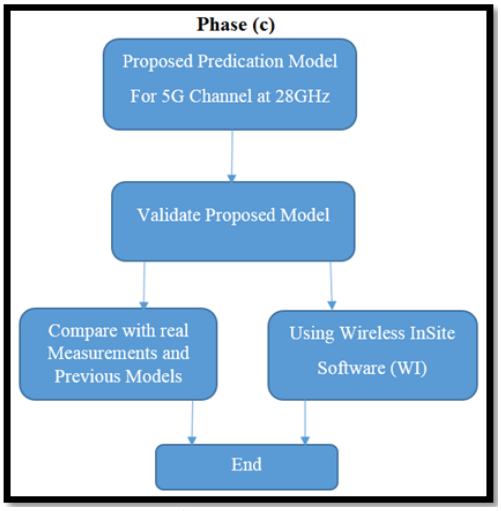

Fig. 9: Flow Chart of Research Methodology - Phase (C).

3.4. Measurement equipment

In this work, a wideband channel sounder system (CSS) was used to conduct the measurement. The measurement equipment is shown in Figure 10. CSS Tx consisted of an Arbitrary Waveform Generator (AWG) (M8190A), up-converter (E8267D) and rubidium clock (FS725). M8190A generated the wideband differential In-phase Quadrature (IQ), i.e., Arbitrary Waveform Channel Sounding (AWCS) signals, which provided 1 ns multipath resolution from a 1000 Mcps Pseudo Random Binary Sequence (PRBS). E8267D up- converted the IQ into RF (up to 40 GHz), and its output was adjusted by E8267D's Automatic Line Controller (ALC) circuit. FS725 synchronized the Tx and Rx, with a 10 MHz reference (< le^{-11} accuracy; < $3e^{-11}$ stability) [31]. The signals were derived from FS725 or 33500B Function Generation. The AWCS Chip Rate was 1000 Mcps, which generated an AWCS signal of l GHz. Tx antennas were placed at a 1.7 m height for emulating the hotspot location, while Rx was placed at the height of 1.5 m.

M9362AD01 Rx down-converted the RF (up to 40 GHz) to an Intermediate Frequency
(IF) that was amplified by M9352A and acquired by a 12-bit M9703A digitizer with a 1 GHz bandwidth. EXG N5173B Analogue signal was the Local Oscillator (LO) of M9362A-D01, while M9300A was a Frequency Reference mode, with external 10 and 100 MHz references. Rx FS725 offered a 10 MHz reference, and the signal was loaded by a 33500B. Horn and Omni direction antennas were used for this work.

Fig. 11: 5G channel sounder system (CSS).

Table 3: CSS-SISO Components for MM-Waves > 6 GHZ

Component	System part	Description
AWG M8190A	Tx	Ultra-wideband AWG sounding signal
PGS E8267D	Tx	5G band (> 6 GHz) signal generator, as Up-converter
EXGN5173B	Rx	5G (> 6 GHz) signal generator, as LO for down-converter
PXIM9362A,	Rx	5G band (> 6 GHz) down-converter, interme-

M9352A and M9300A		diate frequency amplifier and 100 MHz references to M9703A
AXI M9505A	Rx	A wideband 8-channel digitizer for CSS acquisition
FWG 33500B	Tx & Rx	Waveform generator for acquisition triggering signal
FS725	Tx & Rx	Rubidium clock for Tx-Rx synchronization. 10 MHz reference offers a 1 pps I/O with GPS synchronization so that Tx and Rx share a GPS standard time

3.5. Measurement environments

The measurement was carried out at different outdoor environments at the UTM KL campus with the following scenarios:
Scenario 1: Dense LOS without rain. Scenario 2: Open LOS/NLOS without rain. Scenario 3: LOS with rain.
One of the test bed environments for the LOS scenario is shown in Figure 12.

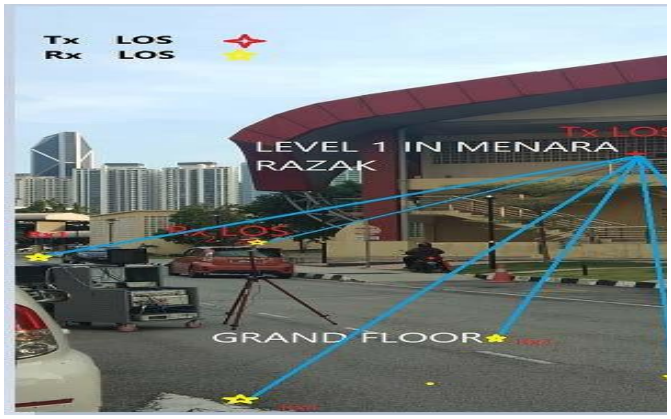

Fig. 13: Measurement environment with A fixed Tx location at 5 M height and different Rx locations with 1.5 height of Rx antenna.

Some of the measurements were conducted in the LOS scenario as shown in Figure 14. The measurements were accrued from the outdoor environment at UTM KL campus. The Tx was fixed with a 5 m antenna height, and the horn antenna was used with a gain of 11.6 dB. The power amplifier was also used with a gain of 24.5 dB. The transmitted power was set to 25 dBm. At the Rx, the horn antenna was used with a gain of 11.6 dB. Moreover, to receive the weak signal from a multipath and far distance, the low noise amplifier (LNA) was used with a gain of 39 dB. The Rx locations are shown in Fig. 3.4. The Rx locations with 3D Tx- Rx separation distance are listed in Table 4

Table 5: Tx-Rx Locations and Distance.

Rx Location	3D Tx-Rx separation distance
Rx 1	24.5 m
Rx 2	22 m
Rx 3	17 m
Rx 4	16.5 m
Rx 5	20 m
Rx 6	30 m
Rx 7	40 m
Rx 8	45 m
Rx 9	50 m
Rx 10	60 m
Rx 11	70 m

3.6. Wireless in site software

WI is a simulation tool used to predict the effect of terrain/ buildings on wave propagation and signal strength. WI models the terrain/ building characteristics used to calculate wave propagation and evaluate the signal characteristics. This was achieved through the following steps:

- Identify System Parameters

Define the parameters for the system such as Antenna specification, Frequency, Waveform, Bandwidth.

- Build system Environment

Build the system Environment and import the environment plan followed by setting the Tx and Rx locations.

- Run Simulation

Before running the simulation, the following parameters need to be defined such as path gain and path loss, Propagation delay, power delay profile and Angle of Arrival.

3.7. 5G channel model parameters

The following parameters were used to investigate PL as a wireless channel characteristic.

- Path Loss

PL represents the inverse of path gain, i.e., amount of signal received. In any narrowband system, PL refers to the decay amount of received power at a specific frequency. For the wideband system, the PL was derived from PDPs by aggregating the MPCs.

- Power Delay Profile

The PDP helps in extracting other parameters such as RMSDS, propagation time delay, number of MPCs.

- RMSDS

The delay characteristics show the distribution of the power relative to the first arriving component. These characteristics are typically quantified regarding root mean square delay spread (RMSD). The RMSD represents the standard deviation value of the delay of reflections and weighted proportionally to the energy in the reflected waves.

- Rain Attenuation

During rainfall, the mm-waves from Tx to Rx get absorbed, scattered, depolarized, and diffracted affecting the mm-wave propagation regarding the attenuation loss, number of PDP multipath profile and their delay.

4. Preliminary results

4.1. Introduction

In this chapter, the preliminary results are presented. The initial results for path loss models, PDPs, MPCs and RMSDS are also discussed.

4.2. Measurement campaign

The measurements were conducted along the road at the back of the Menara Tun Razak Building at the Universiti Teknologi Malaysia (UTM) campus, Kuala Lumpur, Malaysia. The Menara Tun Razak Building is a 17-story building with discussion rooms and faculty offices. The Tx antenna was fixed on the 2^{nd} floor with a height of 5 m from the ground. Two high directional horn antennas were used at Tx and Rx with half power beam width (HPBW) of 39^{o}. The measurement details and figures were previously discussed in Chapter 3 Section 3.5. In the Rx side, some cars were parked beside the road as shown in Figure 15in Chapter 3. The rotator was used at the RX side to rotate the Rx antenna 360^{o} with a 45^{o} step to collect all paths from all directions. This setup was used to emulate the omnidirectional antenna or beam forming technique. In this initial result, the findings were calculated based on the omnidirectional antenna emulator. More investigations based on the beam forming emulator should be undertaken in future.

4.3. Preliminary findings

The path-loss, power delay profile and root mean square (RMS) delay spread analysis were calculated and analyzed. The path loss models, PDP, MPCs and RMS delay spread results and analysis, are discussed in the following subsections.

4.4. Path loss models, results and analysis

In this study, different path loss models were used to investigate the path loss at 28 GHz for the 5G system. The close-in (CI) free space path loss model is a physically based model that uses the free space path loss (FSPL) at 1 m as the reference point to estimate the path loss at different distances and spatial locations. The CI model can be calculated as [57]:

$$P_L{}^{CI}(f,d)[dB] = P_L(f,d_0) + 10n\,log_{10}\left(\frac{d}{d_0}\right) + X_\sigma \quad (4.1)$$

Where $P_L(f,d)$ is the path loss at different frequencies with various Tx-Rx separation distances; n is the path-loss exponent (PLE), $P_L(f,d_0)$ is the path loss in dB at a close-in (CI) distance, d0, of 1 m, and X_σ is a zero-mean Gaussian-distributed random variable with standard deviation σ dB (shadowing effect) [58]. The PLE and minimum standard deviation are derived by the minimum mean square error (MMSE).

Figure 9 shows the scatter plots of the path loss and the CI model for the LOS scenario at 28 GHz. It is shown that the path loss increases as the separation distance increases. The PLE value of 2.9 is found to be more than those of the theoretical free space PLE (n = 2). For the CI model fit as shown in Figure 9, it is noted that the CI model does not fit the measurement data. Hence, the standard deviation value σ is large (21.9 dB).

To make the CI physical based model feasible for this measurement, the modified CI model was proposed with a breakpoint. This proposed model is termed as the close in breakpoint (CIB) model, defined in Eq. 2:

$$P_L{}^{CIB}(f,d)[dB] = \begin{cases} FSPL(f,d_0) + 10n_1\,log_{10}\left(\frac{d}{d_0}\right) + X_\sigma, d < bp \\ FSPL(f,d_0) + 10n_2\,log_{10}\left(\frac{d}{d_0}\right) + X_\sigma, d > bp \end{cases} \quad (4.2)$$

Where, n1 and n2 represent the PLEs value for measurement data before and after breakpoint (bp), respectively. Figure 10 shows the path loss and the CIB model. It can be seen that the CIB path loss model fits the measurement data with PLEs of 0.9 and 3.9 before and after bp (25 m), respectively and the standard deviation values are 1.4 and 5.2 dB for a distance below and above 25 m, respectively. The results from the CIB path loss model indicate that the signal degradation is low until 25 m, then rapid fluctuation in the received signal after 25 m makes the signal drop high; referring to the FSPL at 1 m.

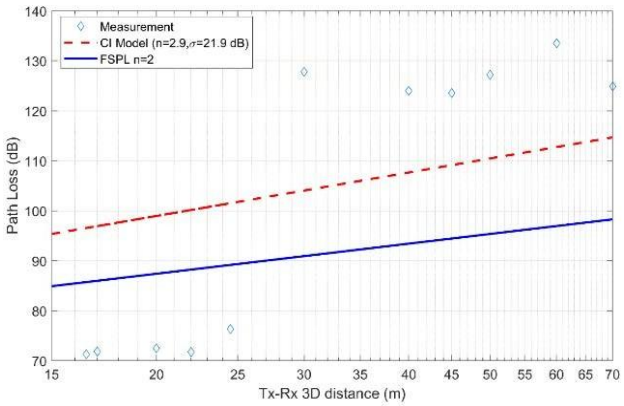

Fig. 16: FSPL and CI (D0 = 1 M) path-loss model for the LOS scenario.

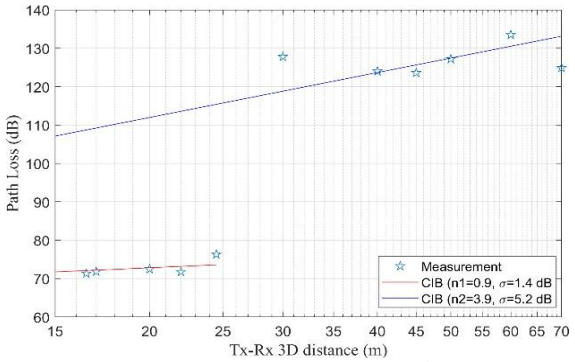

Fig. 17: CIB (D0 = 1 M) Proposed Path-Loss Model for the LOS Scenario.

4.4.1. Power delay profile and delay spread analysis

The received power with different delay along the Tx-Rx separation distance is shown in Figure 11. For all spatial locations along the road, most of the received power arrived at the early excess delay (less than 20 ns). The maximum excess delay is less the 500 ns for all received paths with received power greater than -140 dBm. The received power greater than -80 dBm appears in the directed path (LOS path) that represents the first path in the LOS scenario for the distance less than 30 m. This implies that, when the high directional antenna is used, most power falls in the LOS path. For the MPCs with an excess delay less than 100 ns, the received power in the first five Rx locations is more than -130 dBm. The Rx locations with a distance more than 30 m (Rx 6 to Rx 11), the power is less than -120 dBm; many paths fall in the excess delay of more than 100 ns.

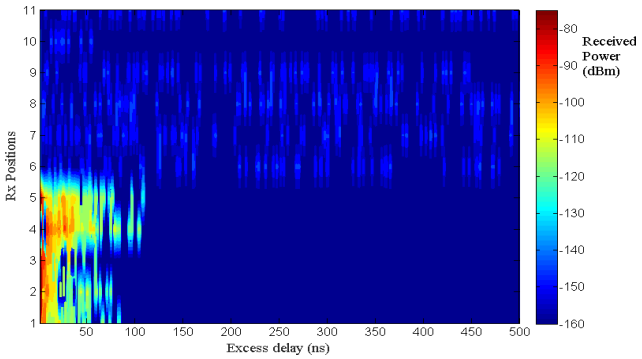

Fig. 18: Received power at different delays in all Tx-Rx separation distances considered for the LOS scenario.

The power delay profiles at some spatial locations are shown in Figure 12, Figure 13 and Figure 14. Figure 12 shows the PDP at the Rx 1 (d = 24.5 m). It can be seen that all MPCs received an excess delay less than 50 ns with a power greater than -120 dBm. The received MPCs at excess delay less than 5 ns have power more than 95 dBm. The PDP at the Rx 5 is shown in Figure 13. It can be seen that all MPCs are received in the excess delay less than 100 ns with received power greater than -140 dBm. The greatest power values are received in the first 5 MPCs with an excess delay less than 5 ns and power greater than -80 dBm.

It is further noted from Figure 13 that most of the MPCs fall in the excess delay range between 30 to 70 ns with received power more than -110 dBm. Figure 12 and Figure 13 present the PDPs for Rx 1 and Rx 2 that have a distance less than a bp of 25 m. The PDPs sample for the Rx location at a distance greater than bp is shown in Figure 14. The PDP for Rx 9 at a distance of 50 m is shown in Figure 14. Here it can be seen that the excess delay reaches until 400 ns; implying that many paths reach with a long propagation time delay. The received power is low compared to the power of Rx 1 and Rx 5. Maximum received power at this location is -143 dB. Moreover, it can be noticed that there was a misalignment of LOS at a direct angle to the Rx, since there are some paths greater than the first path.

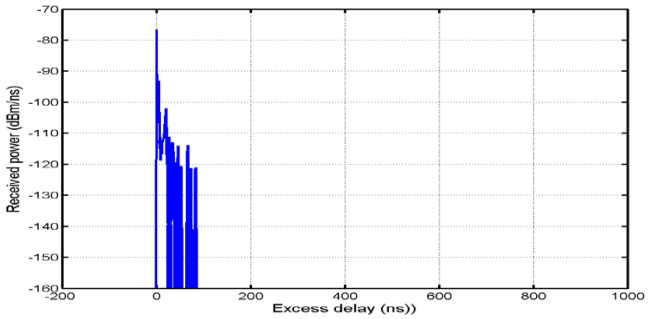

Fig. 19: PDP at Rx 1.

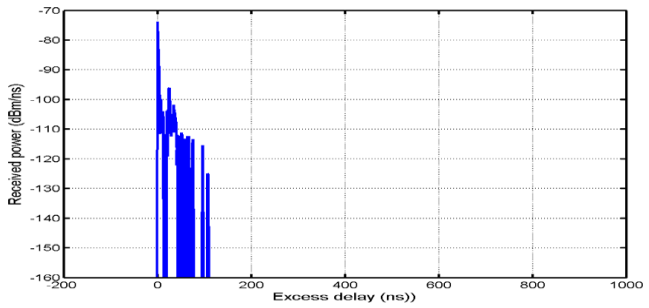

Fig. 13: PDP at Rx 5.

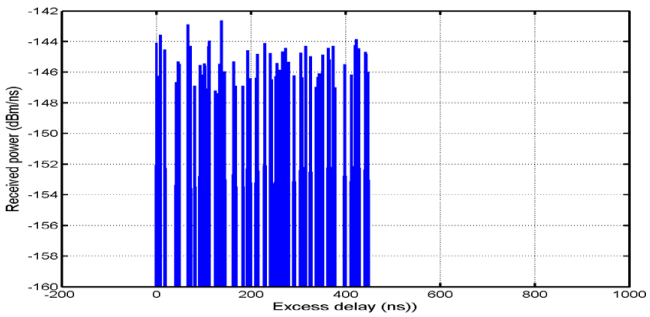

Fig. 14: PDP at Rx 9.

Power delay profiles (PDPs) for different Rx locations.
The RMSDS with Tx-Rx separation distance is shown in Figure 13. It can be seen that the delay spread for all locations less than the proposed bp is less than 10 ns. This implies that most of the MPCs fall in the early bins. For the Rx locations at the bp, it is shown that the delay spread values are in the range between 25 ns and 300 ns.

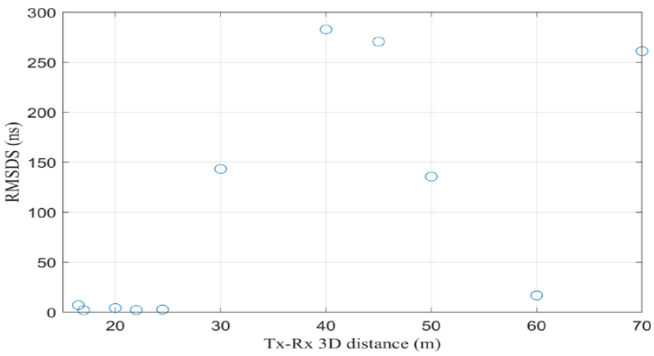

Fig. 15: RMS delay spread (RMSDS) for all Rx locations.

5. Conclusion

In this proposal, the relevant studies for 5G channel studies are reviewed, along with presenting the problem statement and the main aim of the study. The general framework including the measurement and simulation set up were extensively discussed along with presenting the preliminary results based on a number of conducted measurements. The results of this work found that the path loss, power delay profile (PDP), delay and angular spreads from the measurements were found to provide the channel propagation characteristics for 5G wireless networks. Accordingly, the investigation of the rain effect will help to provide useful knowledge and insight for 5G channel behavior with different rain rates. This study successfully produced an accurate 5G channel model for an outdoor environment, which is considered to adequate for the challenges associated with 5G in tropical regions. To validate the proposed model, extensive comparisons of the proposed model, stochastic channel model (performed from measurement and analysis), and simulation (using WI software) were successfully performed. It is proposed that extensive 5G channel measurements and analysis in mobile scenarios at outdoor environments LOS/NLOS be investigated. Based on these measurements and analysis the trend-based model for prediction should be defined. It is proposed that the prediction method be modified based on the comparison with previous models using measurement and WI software.

References

[1] Tudzarov S & Janevski T (2001), Functional architecture for 5G mobile networks, *Int.J. Adv. Sci. Technol.* 32, 65–78.
[2] Kachhavay MG (2014), 5G Technology-evolution and revolution, *Int. J. Comput. Sci. Mob. Comput.*, 3 (3), 1080–1087.
[3] Capacity N (2014), 5G Network Capacity, *IEEE Veh. Technol. Mag.*, 71–78.
[4] Pereira & Sousa T (2004), For more detailed reading and to reference, please use: Vasco Pereira, Tiago Sousa, Paulo Mendes, Edmundo Monteiro, "Evaluation of Mobile Communications: From Voice Calls to Ubiquitous Multimedia Group Communications ", in Proc. of the 2nd Intern," *Evol. Mob. Commun. from 1G to 4G Vasco*, 1–7.
[5] Lee H, Vahid S & Moessner K (2014), A survey of radio resource management for spectrum aggregation in LTE-advanced," *IEEE Commun. Surv. TUTORIALS*, 16 (2), 745–760, available online: https://doi.org/10.1109/SURV.2013.101813.00275, last visit: 25.12.2018
[6] In O (2011), An introduction to millimeter-wave mobile broadband systems, 101–107, available online: https://doi.org/10.1109/MCOM.2011.5783993, last visit: 2.01.2019
[7] Sun S, Rappaport TS, Thomas TA, Ghosh A, Nguyen HC & Kov IZ (2016), Investigation of prediction accuracy, sensitivity, and parameter stability of large-scale propagation path loss models for {5G} wireless communications, *IEEE Trans. Veh. Technol.*, 65 (5), 1–18, available online: https://doi.org/10.1109/TVT.2016.2543139, last visit: 5.010.2018.
[8] Liu D, Wang L, Chen Y & Elkash-lan M (2016), User association in 5G networks: A survey and an outlook, *IEEE Commun. Surv. Tutorials*, 18 (2), 1018–1044, available online: https://doi.org/10.1109/COMST.2016.2516538, , last visit: 8.12.2018.
[9] Xu H, Member S, Rappaport TS, Boyle RJ & Schaffner JH (2000), Measurements and models for 38-GHz point-to-multipoint radiowave Propagation, *IEEE J. Sel. AREAS Commun.*, 18 (3), 310–321.
[10] Ghosh A, Thomas TA, Cudak MC, Ratasuk R, Moorut P, Vook FW, Rappaport TS, MacCartney GR, Sun S & Nie S (2014), Millimeter-wave enhanced local area systems: A high-data-rate approach for future wireless networks," *IEEE J. Sel. AREAS Commun.*, 32 (6), 1152–116.
[11] Talwar S, Choudhury D, Dimou K, Aryafar E, Bangerter B & Stewart K (2014), Enabling technologies and architectures for 5G wireless, *IEEE MTT-S Int. Microw. Symp.*, https://doi.org/10.1109/MWSYM.2014.6848639.
[12] Rappaport TS, Xing Y, Member S, Maccartney GR & Molisch AF (2017), Overview of millimeter wave communications for a focus on propagation models, *IEEE Trans. Antennas Propag.*, 65 (12), 6213–6230, https://doi.org/10.1109/TAP.2017.2734243.
[13] Series M (2015), IMT vision – framework and overall objectives of the future development of IMT for 2020 and beyond, *Recomm. ITU-R M.2083-0*, 1-21.
[14] Kar UN & Sanyal DK (2018), A sneak peek into 5G communications, *Spring Elsavier*, 5, 555–572.
[15] Hossain E & Hasan M (2015), 5G cellular: key enabling technologies and research challenges, *IEEE Instrum. Meas. Mag.*, 6, 11–21.
[16] Fletcher S & Telecom NEC (2014), Cellular architecture and key technologies for 5g wireless communication networks," *IEEE Commun. Mag.*, 2, 122– 130.

[17] Roh W, Seol JY, Park JH, Lee B, Lee J, Kim Y, Cho J & Cheun K (2014), Millimeter-wave beamforming as an enabling technology for 5G cellular communications: Theoretical feasibility and prototype results, *IEEE Commun. Mag.*, 52 (2), 106–113.

[18] Kutty S & Sen D (2016), Beamforming for millimeter wave communications: an inclusive survey," *IEEE Commun. Surv. Tutorials*, https://doi.org/10.1109/COMST.2015.2504600.

[19] Molisch AF (2009), Ultra-wide-band propagation channels, *IEEE Xplore.*, 97 (2), 353–371.

[20] Akyildiz F, Gutierrez-estevez DM, Balakrishnan R & Chavarria-reyes E (2014), LTE-advanced and the evolution to beyond 4G (B4G) systems, *Phys. Commun.*, 10, 31–60.

[21] Zhao H, Mayzus R, Sun S, Samimi M, Schulz JK, Azar Y, Wang K, Wong GN, Gutierrez F & Rappaport TS (2013), 28 GHz millimetre wave cellular communication measurements for reflection and penetration loss in and around buildings in New York City, *IEEE Int. Conf. Commun.*, 5163–5167.

[22] Azar Y, Wong GN, Wang K, Mayzus R, Schulz JK, Zhao H, Gutierrez F, Hwang DD & Rappaport TS (2013), 28 GHz propagation measurements for outdoor cellular communications using steerable beam antennas in New York city, *IEEE ICC - Wirel. Commun. Symp.* 28, 5143–5147.

[23] Samimi M, Wang WK, Mayzus R, Schulz JK, Sun S, Gutierrez F, Hwang DD & Rappaport TS (2013), 28 GHz angle of arrival and angle of departure analysis for outdoor cellular communications using steerable-beam antennas in New York City, *Proc. IEEE Veh. Technol.* 1–6.

[24] Rappaport TS, Sun S, Mayzus R, Zhao H, & Schulz JK (2013), Millimeter-wave mobile communications for 5G Cellular: It will work! *IEEE Access*, 1, 335–349.

[25] Sulyman A, Nassar M, Samimi G, Maccartney GR, Rappaport T & Alsanie A (2014), Radio propagation path loss models for 5G cellular networks in the 28 GHz and 38 GHz millimetre-wave bands, *IEEE Commun. Mag.*, 52 (9), 78–86, https://doi.org/10.1109/MCOM.2014.6894456.

[26] Nie S, MacCartney GR, Sun S & Rappaport TS (2014), 28 GHz and 73 GHz signal outage study for millimeter wave cellular and backhaul communications, *IEEE Int. Conf. Commun. ICC*, 4856–4861.

[27] Akdeniz MR, Liu Y, Samimi MK, Sun S, Rangan S & Rappaport TS (2014), Millimeter wave channel modeling and cellular capacity evaluation, *IEEE J. Sel. Areas Commun.*, 32 (6), 1164–1179.

[28] Deng S, Slezak CJ, Jr GRM & Rappaport TS (2014), Small wavelengths - big potential: millimeter wave propagation measurements for 5G, *Microw. J.*, 57 (11), 4–12.

[29] Sun S, MacCartney GR & Rappaport TS (2016), Millimeter-wave distance-dependent large-scale propagation measurements and path loss models for outdoor and indoor 5G systems, *10th Eur. Conf. Antennas Propagation, EuCAP 2016*, https://doi.org/10.1109/EuCAP.2016.7481506, last visit: 3.01.2019.

[30] Kim MD, Liang J, Lee J, Park J & Park B (2016), Directional multipath propagation characteristics based on 28GHz outdoor channel measurements, *10th Eur. Conf. Antennas Propagation, EuCAP 2016*.

[31] Al-Samman M, Rahman TA, Azmi MH & Hindia MN (2016), Large-scale path loss models and time dispersion in an outdoor line-of-sight environment for 5G wireless communications, *AEU - Int. J. Electron. Commun.*, 70 (11), 1515–1521.

[32] Ko J, Lee K, Cho YJ, Oh S, Hur S, Kang N, Park J, Park DJ & Cho DH (2016), Feasibility study and spatial–temporal characteristics analysis for 28 GHz outdoor wireless channel modelling, *IET Commun.*, 10 (17), 2352–2362.

[33] Rajagopalan R & Hoffman M (2016), path loss analysis in millimeter wave cellular systems for urban mobile communications, *Proc SPIE*, 9977, 1–7.

[34] Naderpour R, Vehmas J, Nguyen S & Jan J (2016), spatio-temporal channel sounding in a street canyon at 15, 28 and 60 GHz, *2016 IEEE 27th Annu. IEEE Int. Symp. Pers. Indoor Mob. Radio Commun. - Fundam. PHY*, https://doi.org/10.1109/PIMRC.2016.7794730.

[35] Wang G, Liu Y, Li S, Zhang X & Chen Z (2016), study on the outdoor wave propagation at 28ghz by ray tracing method, *IEEE Access*.

[36] Tuan M, Cheon Y, Aoki Y & Kim Y (2016), Performance comparison of millimeter-wave communications system with different antenna beamwidth, *IEEE Commun. Mag.*

[37] Lee M, Kim J, Liang J, Park T & Park B (2016), Frequency range extension of the itu-r nlos path loss models applicable for urban street environments with 28 ghz measurements, *IEEE Antennas Propag. Mag.*

[38] Hur S, Baek S, Kim B, Chang Y, Molisch AF & Rappaport TS (2016), Proposal on millimeter-wave channel modeling for 5G cellular system, *IEEE J. Sel. Top. Signal Process*, https://doi.org/10.1109/JSTSP.2016.2527364.

[39] Parameter M, Path S & Data L (2016), 5G Millimeter-wave channel model alliance parameter, and measured path loss data measurement parameter, scenario list, *NYU Wirel. TR 2016-002 Tech. Rep. 5G*.

[40] Tang P, Tian L & Zhang J (2017), Analysis of the millimeter wave channel characteristics for urban micro-cell mobile communication scenario, *IEEE Antennas Propag. Mag.*, 2880–2884, https://doi.org/10.23919/EuCAP.2017.7928207.

[41] Park J, Lee J, Liang J, Kim K, Lee K & Kim M (2017), Millimeter wave vehicular blockage characteristics based on 28 ghz measurements, *IEEE 86th Veh. Technol. Conf.*, 1–5.

[42] Khatun S, Mehrpouyan H, Matolak D & Guvenc I (2017), Millimeter wave systems for airports and short-range aviation communications: a survey of the current channel models at mmwave frequencies, *IEEE Digit. Avion.*, https://doi.org/10.1109/DASC.2017.8102042, last visit: 11.12.2018.

[43] Bas CU, Wang R, Sangodoyin S, Hur S, Whang K, Park J & Zhong J (2018), 28 GHz propagation channel measurements for 5G microcellular environments, *International Applied Computational Electromagnetics Society Symposium in Denver, ACES-Denver 2018*, 0–1. https://doi.org/10.23919/ROPACES.2018.8364139.

[44] Zhong Z, Li C, Zhao J & Zhang X (2017)., Height-dependent path loss model and large-scale characteristics analysis of 28 ghz and 38. 6 ghz in urban micro scenarios, *IEEE Antennas Propag. Mag.*, 1818–1822.

[45] Nur Azhari I, Aziz OA, Din J & Rahman TA (2017), Modelling impact of topography gradient on signal path loss along the roadway for 5g, *J. Electr. Eng.*, 16 (2), 11–15.

[46] Zhou L, Xiao L, Yang Z & Li J (2017), Path loss model based on cluster at 28 GHz in the indoor and outdoor environments, *Sci. China Press Springer-Verlag Berlin Heidelb*, 60 (8), 1–11.

[47] Wei S, Ai B, He D, Guan K, Wang L & Zhong Z (2017), Calibration of ray-tracing simulator for millimeter-wave outdoor communications, *IEEE Int. Symp. Antennas Propag. Usn. Natl. Radio Sci. Meet.*, 1, 1907–1908, https://doi.org/10.1109/APUSNCURSINRSM.2017.8072996.

[48] Zhao K, Gustafson C, Liao Q, Zhang S & Bolin T (2017), Channel characteristics and user body effects in an outdoor urban scenario at 15 and 28 GHz, *6534 IEEE Trans. ANTENNAS Propag.*, 65 (12), 6534–6548.

[49] Hindia MN, Al-samman AM, Rahman TA & Yazdani TM (2018), Outdoor large- scale path loss characterization in an urban, *Phys. Commun.*, 27, 150–160.

[50] Lodro MM, Majeed N, Khuwaja AA, Sodhro AH & Greedy S (2018), Statistical channel modelling of 5G mmWave MIMO wireless communication, *International Conference on Computing, Mathematics and Engineering Technologies (iCoMET)*, 1–5.

[51] Jarndal S & Alnajjar K (2018), MM-wave wideband propagation model for wireless communications in built-up environments, *Phys. Commun.*, 28, 97–107.

[52] Ko J, Hur S, Lee S, Kim Y, Noh YS, Cho YJ, Kim S, Bong S, Park J, Park DJ & Cho DH (2018), 28 GHz channel measurements and modeling in a ski resort town in pyeongchang for 5g cellular network systems, *IEEE Xplore*.

[53] Lee J, Choi J, Kim S & Member S (2018), Cell coverage analysis of 28 ghz millimeter wave in urban microcell environment using 3-d ray tracing, *IEEE Trans. Antennas Propag.*, 66 (3), 1479–1487.

[54] Lee J, Kim M, Park J & Chong YJ (2018), Field-measurement-based received power analysis for directional beamforming millimeter-wave systems: effects of beamwidth and beam misalignment, *Journal Wiley Online Libr.*, 40 (1), 26–38.

[55] Karttunen A, Järveläinen J & Le Hong S (2018), Modeling the multipath cross- polarization ratio for above-6 ghz radio links, *IEEE Antennas Propag. Mag.*, 671650, 1–20.

[56] Sheikh MU & Lempiainen J (2018), Analysis of outdoor and indoor propagation at 15 ghz and millimeter wave frequencies in microcellular environment analysis of outdoor and indoor propagation at 15 ghz and millimeter wave frequencies in microcellular environment, *Adv. Sci. Technol. Eng. Syst. J.*, 1-13.

[57] MacCartney GR, Member S, Rappaport TS, Sun S & Deng S (2015), Indoor office wideband millimeter-wave propagation measurements and channel models at 28 and 73 GHz for Ultra-Dense 5G Wireless Networks, *IEEE Access*, 3 (c), 2388– 2424.

[58] Rappaport TS (2002), *Wireless Communications Principles and Practice*, 2nd ed. Up. Saddle River, NJ Prentice Hall.